

SRL
RECORD COPY

SRL
RECORD COPY

RECORDS ADMINISTRATION



ACBT

DP-MS-75-62

ACC#738299

THERMAL CONDUCTIVITY OF $^{238}\text{PuO}_2$ POWDER,
INTERMEDIATES, AND DENSE FUEL FORMS

by

D. F. Bickford and B. Crain, Jr.

Savannah River Laboratory
E. I. du Pont de Nemours and Co., Inc.
Aiken, South Carolina

A paper proposed for presentation to the
Fall Meeting of the Nuclear Division of the
American Ceramic Society in Seattle, Washington,
October 29-31, 1975

This paper was prepared in connection with work under Contract No. AT(07-2)-1 with the U. S. Energy Research and Development Administration. By acceptance of this paper, the publisher and/or recipient acknowledges the U. S. Government's right to retain a nonexclusive, royalty-free license in and to any copy-right covering this paper, along with the right to reproduce and to authorize others to reproduce all or part of the copy-righted paper.

THERMAL CONDUCTIVITY OF $^{238}\text{PuO}_2$ POWDER,
INTERMEDIATES, AND DENSE FUEL FORMS[†]

D. F. Bickford and B. Crain, Jr.

Savannah River Laboratory
E. I. du Pont de Nemours and Co., Inc.
Aiken, SC 29801

ABSTRACT

The thermal conductivities of porous $^{238}\text{PuO}_2$ powder (calcined oxalate), milled powder, and high density granules were calculated from direct measurements of steady-state temperature profiles resulting from self-heating. Thermal conductivities varied with density, temperature, and gas content of the pores. Errors caused by thermocouple heat conduction were less than 5% when the dimensions of the thermal conductivity cell and the thermocouple were properly selected.

[†] The information contained in this article was developed during the course of work under Contract No. AT(07-2)-1 with the U.S. Energy Research and Development Administration.

Introduction

A blend of plutonium oxide isotopes, 80% $^{238}\text{PuO}_2$ - 20% $^{239}\text{PuO}_2$ (hereafter called PuO_2), has been produced at the Savannah River Plant (SRP) from calcined plutonium oxalate since 1961. The high heat generating rate (≈ 0.4 watts/g) and relatively low amount of penetrating radiation make the blend an ideal source of heat for thermoelectric generating systems.

The PuO_2 has been converted into fuel forms for various applications at Mound Laboratory. A cermet fuel (PuO_2 -molybdenum) has been used for power systems in the Transit, Pioneer, Viking, and Mars Lander Programs. More recently, hot-pressed PuO_2 spheres are being developed for use at higher operating temperatures in systems for instrument power in the Lincoln Experimental Satellite (LES).

The high power generation rate of PuO_2 coupled with low thermal conductivities of intermediate products introduced in the process [1] produced substantial steady-state temperature gradients. Such gradients must be controlled to minimize deleterious effects on sinterability, $^{16}\text{O}_2$ isotopic enrichment (to minimize neutron emission), stoichiometry, and impurity phase transport.

The thermal conductivity of powder depends on both the thermal diffusivity of the PuO_2 itself and the conductivity in pores and between particles. Ondracek and Schulz [2] analyzed the thermal conductivity of porous ceramic bodies having negligible heat transfer in the pore phase. Tennery demonstrated [3],

however, that heat conduction in 82% theoretical density PuO₂ is controlled by the gas phase present in the pores, making Ondracek and Schulz's model unapplicable. Other models with significant pore conductivity [4] require knowledge of the pore configuration, which is not known for the powdered forms of PuO₂.

Because of these factors and the factor of ten difference in conductivities of the gases and solid phases, the conductivity was measured experimentally. The results of the measurements on arrays of powder and granules are presented, and the data are compared with various models. Previous measurements of the conductivity of sintered bodies are also re-evaluated with respect to these models.

Thermal Conductivity of Dense PuO₂

Although the thermal conductivity of UO₂-PuO₂ solid solution has been measured [5,6], Lagedrost et al. [7] made the only high temperature measurement of thermal diffusivity or conductivity of pure plutonium dioxide. Thermal diffusivities were measured ~~at~~ ~~in~~ between 300°C and 1200°C on pellets of 96.5% and 81.9% theoretical density. Thermal conductivities were then calculated by assuming the unmeasured heat capacity of PuO₂ to be identical to that of UO₂ through use of the equation:

$$K = \alpha \rho C_p \quad (1)$$

where:

$$K = \text{thermal conductivity (cal/sec-cm-}^\circ\text{C)}$$

α = thermal diffusivity (cm²/sec)

ρ = density (g/cc)

C_p = specific heat (cal/g °C)

The calculated thermal conductivity was then divided by (1 - volume fraction of pores) to correct the data to theoretical density.

The heat capacity of PuO₂ has been subsequently measured by Kruger and Savage [8], and recalculations of the Lagedrost data [7] for this value of C_p are given in Tables 1 and 2.

Samples prepared at the Savannah River Laboratory (SRL) under conditions similar to those discussed in Reference 7 exhibit finely divided spherical porosity. Assuming spherical porosity with negligible heat conduction in the pores, Maxwell's equation [9] may be arranged to obtain a more exact correction factor for these low porosity samples:

$$K = \frac{K_s (1 + 0.5P)}{1 - P} \quad (2)$$

where:

K = thermal conductivity of theoretically dense material

K_s = thermal conductivity of sample

P = porosity of sample

The results of applying this correction factor to calculate the thermal conductivity of 100% theoretically dense PuO₂ are also shown in Table 1.

The maximum combined error in the original work caused by the use of the heat capacity of UO₂ and the simplified correction for nontheoretical density is 20%.

Maxwell's equation cannot be applied at high porosity levels because of pore-to-pore interactions [4,10]. Nevertheless, the thermal conductivities of theoretically dense PuO₂ calculated by this method from the measured thermal diffusivities of samples of 96.5% and 81.9% theoretical density are within experimental error at temperatures above 700°C (Fig. 1).

Niesel [11] developed an equation for spherical pores with negligible conductivity that is free of the high porosity restriction and which reduces to:

$$K_{100\% \text{ TD}} = K_{\text{sample}} (1 - P)^{3/2} \quad (3)$$

where TD = theoretical density. As is shown in Figure 1, however, Maxwell's equation yields more satisfactory values for K_{TD} for samples of 81.9% of theoretical density than Niesel's equation.

The decrease in thermal conductivity of 96% TD PuO₂ with temperature closely approximates the expected 1/T relationship for ceramics above their Debye temperatures (Fig. 2). The 100% TD curve shows similar behavior, because it was derived from the 96% TD data. The thermal diffusivity curve for the PuO₂ of 81.9% theoretical density data also shows the 1/T relationship, albeit the conductivity is lower because of the porosity.

Calculation of Thermal Conductivity from Self-Heat

Fourier's equation for heat transfer may be simplified for a sphere to:

$$1/r^2 \frac{d}{dr} \left(r^2 K \frac{dT}{dr} \right) = -S_o \quad (4)$$

where:

S_o = the volumetric heat generation rate

K may be a function of T , ρ , etc.

The solution to Equation (4) is subject to the assumption that there is only radial heat flow, leading to the first boundary condition (i) where surface temperature (T_s) is constant. Further, in this system, S_o is limited because it is a function only of density (i.e., the density is assumed constant and there are no singularities in the heat source term), and a second boundary condition may be derived (ii) where the temperature gradient at the geometrical center ($dT/dr|_c$) is zero. Rearrangement and integration of Equation (4) yields:

$$Kr^2 \frac{dT}{dr} = - \frac{S_o r^3}{3} \quad (5)$$

Upon further rearrangement and integration:

$$\int_{T_c}^{T_s} K dT = - \frac{S_o}{3} \int_0^R r dr = \frac{S_o R^2}{6} \quad (6)$$

where:

K is not assumed to be constant.

Because the volume specific heat generation rate is proportional to density, and K_{sample} is approximately equal to the relative density times K at theoretical density, local density variations can be shown to have minimal effects on temperature distribution [3].

Similar solution methods have been used to deduce thermal conductivity from in-reactor experiments [12]. The thermal conductivity of curium oxide powder was estimated by measuring the difference in surface and centerline temperatures caused by self-heat when the powder was held in a cylindrical container [13]. More recently, Tennery assumed K to be constant over a range, and used this same technique to calculate the thermal conductivity of spheres of $\approx 80\%$ TD that were hot-pressed from PuO_2 [3]. In this paper, a polynomial $K(T)$ was substituted with Equation 6, and coefficients were determined by least squares fit.

Measurements with Fixed Thermocouples

Temperatures within spherical thermal-conductivity cells were measured with fixed thermocouples. These cells consisted of 1.5-in. (3.8 cm) diameter, spherical, *Pyrex* (Corning Glass Works, Corning, New York) flasks, each containing two 0.003-in. (0.0762 mm) iron-constantan thermocouples (Fig. 3). The first thermocouple extended across the diameter of the sphere with its hot junction at the sphere's center; the second thermocouple had its hot junction in contact with the surface of the powder. The spherical portion of the cell was coated with ≈ 0.01 in. (≈ 0.25 mm) of refractory cement to prevent short-circuiting of the thermocouple and was surrounded by copper shot in a 500-ml, stainless-steel beaker. Copper shot was used to minimize temperature variations around the surface of the sphere, boundary condition (i). The entire assembly was placed in a muffle furnace so the temperature

of the powder surface in the conductivity cell could be controlled by adjusting furnace temperature. The furnace was purged with helium, air, or argon to provide measurements of the effect of the gas content within the pores (Table 3). Higher temperature measurements for ball-milled powder were made possible by using a similar conductivity cell made from fused silica, with 0.003-in. diameter, Pt/Pt-Rh thermocouples.

Measurements were made on three types of powder (Table 4). The first powder was calcined, reverse-strike plutonium oxalate, typical of current SRP production (Fig. 2). The oxalate is precipitated by adding plutonium(III) nitrate to oxalic acid. The medium particle size was 5 μm as measured by a *Coulter Counter* instrument (Coulter Electronics, Hialeah, Florida), and individual particles are typically plates with an aspect ratio of 1:5:15 (thickness:width:length). The second powder investigated was similar powder that was ball-milled to reduce the median particle size to 2 μm . Also investigated were high-density granules of 53 to 500 μm in diameter that were made by cold-pressing the ball-milled powder at 58,000 psi, breaking the resulting pellet into granules, and sintering the granules at 1650°C for 10 hours.

Measurements with Movable Thermocouples

A second method permitted direct measurement of the temperature gradient across a spherical array of powder or granules. Aluminum cylinders, 2.5-in. (6.35 cm) diameter by 2.5-in. high, with 1-in. (2.54 cm) or 1.25-in. (3.17 cm) spherical cavities

(Fig. 3), were filled with PuO₂ and allowed to reach steady-state temperature. To measure the temperature gradient within a cylinder, the hot junction of a Pt/Pt-Rh thermocouple was moved along a diameter of the spherical cavity, and temperatures were measured as a function of distance from the center (radius). Differentiating a polynomial least squares fit of the temperature vs. radius yields $\partial T/\partial r = f(r)$, and substituting this expression into Equation (5) yields $K_{\text{sample}} = f(T)$.

Thermal Conductivity of Dense PuO₂

Experimentally measured surface and center temperatures of hot-pressed PuO₂ spheres (~80% TD) at Los Alamos Scientific Laboratory (LASL) and Mound Laboratory have been analyzed to obtain conductivity values [3]. These values are for spheres in atmospheres of helium, vacuum, and argon saturated with water and at surface temperatures ranging from 300 to 1400°C. The implicit assumption that K is constant over a moderate range (<277°C) permitted comparison of K with T, leading to Tennery's conclusion that heat transfer at this density is dominated by the gas phase present in the pores with the thermal conductivity varying as $(T, \text{ }^\circ\text{K})^{1/2}$, and that a simple model of parallel gas slabs and oxide slabs with heat conduction perpendicular to the slabs is adequate. More properly $K = f(T)$. For series heat flow, Equation 5 becomes:

$$\frac{dT}{dr} = \left(\frac{-S_{0r}}{3} \right) / \left(\frac{K_s K_g}{PK_s + (1-P)K_g} \right) \quad (7)$$

With the exception of measurements for Sphere SPP-59 in Ar-H₂O (Fig. 1), the conductivity data fall between the conductivities of PuO₂ at 100% TD and the gas phase present in the pores. Further, the conductivity is generally proportional to the conductivity of the gas phase present. The behavior of Sphere SPP-59 in Ar-H₂O appears anomalous when compared to the behavior of Sphere SPP-60. Analysis by Tennery, based upon the thermal conduction of a classical gas, led to the conclusion that the gas-mixture in Sphere SPP-59 has 50 degrees of freedom, i.e., a very large thermal conductivity [3]. The argon was saturated with water at room temperature, and it is not apparent how the relatively minor amount of water present could so drastically increase the relatively low conductivity of argon to a level exceeding the value for helium.

The reason for the variation of conductivity of hot-pressed spheres with temperature is illustrated in Fig. 2, which shows the microstructure of a hot-pressed pellet produced at SRL using the same flowsheet as was used for the PuO₂ in Spheres SPP-59 and SPP-60. The sphere consists of the high-density remnants of the granules from which it was hot pressed. Each granule is almost totally surrounded by voids, with relatively small necks linking the granules. At low temperatures, $K_{\text{gas}} \ll K_{\text{solid}}$, and most of the heat conducted must pass through the necks. Thus, the small necks, which possess a high thermal resistance because of their small area, produce the low overall conductivity of the body. At

intermediate temperatures, the gas has sufficient conductivity to short-circuit the high neck resistance and thereby permit moderate conductivities approaching the theoretically dense solid. Because the solid and gas phases form two separate connected and inter-laced phases at very high temperatures (where $K_{\text{gas}} \gg K_{\text{solid}}$), the process is expected to be analogous to that of very low temperatures with the roles of the solid and gas reversed, if thermal radiation is ignored.

Microstructural analysis of typical hot-pressed PuO_2 permits the replacement of K_{solid} in Equation 7 by a polynomial fitted to the values in Table 1 for PuO_2 of 96.5% TD, and K_{gas} [14] may be replaced by a similar polynomial. Numerical integration leads to the calculated temperatures at the sphere centers that are listed in Table 3. As may be seen by comparing the calculated and actual values, the series slab model is acceptable for PuO_2 in helium, but unacceptable for argon where $K_{\text{gas}} \ll K_{\text{solid}}$.

Thermal Conductivity of PuO_2 Powder in Argon

The conductivity of ball-milled PuO_2 in argon nearly parallels that of the gas phase and increases with the packing fraction of PuO_2 (Fig. 4).

The conductivity vs temperature curve for as-calcined PuO_2 powder ($\rho = 1.12 \text{ g/cc}$) is a linear least squares fit of three data points. The lack of more data points and the relatively small range of temperatures over which the measurements were made are probable causes of the slope deviating from that of the other powders.

Thermal Conductivity of PuO₂ Powder in Air

Similar to the measurements in argon discussed above, the thermal conductivity of PuO₂-air mixtures increases with the packing fraction of PuO₂, and the variation in conductivity with temperature parallels that of the gas phase (Fig. 5).

The measurements made on the granules and the as-calcined ($\rho = 1.528$) powder were made using the moving thermocouple technique. The sharp inflections of the conductivity vs temperature curves of these two samples at high temperature are discussed in the experimental error section below.

Thermal Conductivity of Ball Milled PuO₂ Powder in Helium

Helium offers an unique opportunity to test various thermal conductivity mixture models; its conductivity is approximately 10 times that of argon, and at $\sim 670^\circ\text{C}$ is 0.1 that of PuO₂. By all rules of mixture (series slab flow, parallel slab flow, combinations of series and slab flow, etc.), the thermal conductivities of all possible mixtures should fall between those of the components. The fact that the experimental curves pass below the intersection (Fig. 6) indicates that other effects, heretofore not considered, must be included in any complete model. Thermal radiation, convection, and other alternative paths of heat transfer can be eliminated because they would tend to increase the overall thermal conductivity of the mixture, thereby making the curves pass above the intersection point. Rather, this phenomenon can only be explained by a mechanism

which adds resistance, such as a film heat-transfer coefficient which limits heat transfer through the solid/gas interfaces. indicates that other effects, heretofore not considered, must be included in any complete model. Thermal radiation, convection, and other alternative paths of heat transfer can be eliminated because they would tend to increase the overall thermal conductivity of the mixture, thereby making the curves pass above the intersection point. Rather, this phenomenon can only be explained by a mechanism which adds resistance, such as a film heat-transfer coefficient which limits heat transfer through the solid/gas interfaces.

Experimental Errors

One error is proportional to the deviations from sphericity of the cavity of the thermal conductivity cell. For the aluminum cells, this was controlled to less than 0.2% by the 0.001-in. tolerance on the 1.000-in. and 1.250-in. diameter cavities. For glass and fused silica cells, the deviations were controlled to less than 5% by using selected hand-blown flasks.

For fixed thermocouple measurements, the hot-junction bead may be rather large, and the junction need only be located near the center within $\pm 5\%$ of the radius, since $\partial T/\partial r = 0$ at the center of the sphere (Fig. 7). The location of the thermocouple used to measure surface temperature is much more critical, as it is located near where $\partial T/\partial r$ is greatest.

The boundary condition ($T_{\text{surface}} = \text{constant}$) about the

surface must be satisfied. The use of a massive aluminum cylinder for the movable thermocouple measurements assured that the range was held to less than 3°C. Although not measured for the glass and fused silica thermal conductivity cells, the copper shot surrounding the flask is assumed to have held the range to less than 5°C. By comparison, surface temperature variations of greater than 15°C are typical for free-standing, hot-pressed spheres. Because total temperature gradients may be less than 75°C for hot-pressed spheres at elevated temperatures, errors of about 20% may be expected.

The thermocouple penetrating the material must be as small as possible to minimize temperature measurement errors. The total effect of the thermocouple can be divided into two factors. The first factor is power dilution. The true heat flux at a radius, r , can be determined by the equation:

$$4\pi r^2 q(r) = S_0 \frac{4}{3}\pi r^3 - 2 A_t r \quad (8)$$

where A_t is the cross-sectional area of the thermocouple. With a small thermocouple, A_t becomes important only when the movable thermocouple method is used, and then only near the center of the sphere. The second factor is thermal short-circuiting of the thermocouple. Thermocouples, because of their relatively high thermal conductivity, tend to make the measured temperature gradients less than the gradients which would exist in the absence of a thermocouple. This effect is least where $\partial T/\partial r$ is least (i.e., near the center of the sphere) and greatest where $\partial T/\partial r$ is

greatest (i.e., near the sphere's surface). Calculating the amount of error caused by this effect is not generally possible, as it is necessary to know the thermal conductivities as a function of temperature for both the thermocouple and the material whose temperature is being measured, as well as the film heat-transfer coefficient between the thermocouple and the surrounding material.

These errors, however, may be estimated by comparing the temperature profiles for identical samples with different diameter thermocouples. The temperature profiles of PuO_2 granules in air as measured by three different diameter thermocouples are shown in Figure 7. Assuming that the total error of the measured temperatures is proportional to cross-sectional area of the thermocouple, then the approximate errors may be expressed as percentages of the total measured gradients (Table 5).

Errors of temperature recorded for hot-pressed spheres and powder measured with similar thermocouples and dimensions may be assumed to be similar, since the conductivities of the thermocouples are 100 times higher than those of any of the PuO_2 -gas mixtures investigated. Because of mechanical handling considerations, minimum practical diameters for thermocouples are 0.003-in. diameter for fixed thermocouple measurements, and 0.005-in. diameter for measurements by the movable thermocouple method.

Measurements with movable thermocouples are more sensitive to displacement from the true center of the sphere than fixed thermocouple measurements; i.e., for a traveling thermocouple not actually passing through the center of the sphere, the assumed heat flux used is less than actual, resulting in the calculation of lower than actual thermal conductivities (c.f. as calcined powder, $\rho = 1.528$ in air, Fig. 5).

Summary

1. The thermal conductivity of PuO_2 calculated from Lagedrost's thermal diffusivity measurements on samples of 96.5% and 81.9% theoretical densities varies approximately as $1/T$, in agreement with single phase ceramic conduction theory.
2. Maxwell's equation is applicable to PuO_2 powder hot pressed to densities between 80 and 100% of theoretical density.
3. Granulation of PuO_2 powder prior to hot pressing produces complicated pore structures requiring a more complicated mixture theory than that of Maxwell.
4. For powders with open porosity filled with a gas phase where $K_{\text{gas}} \ll K_{\text{solid}}$, the conductivity of the mixture falls between that of the solid and the gas, parallels the conductivity of the gas with temperature, and is proportional to the volume fraction of solid.
5. For hot-pressed microstructures with low solid-phase connectivity, the series-slab, heat-flow model is applicable where $K_{\text{gas}} \approx K_{\text{solid}}$. On the other hand, mixing models for powder predict higher than actual conductivities at $K_{\text{gas}} \approx K_{\text{solid}}$, indicating that another source of resistance is required in the models, such as a film heat-transfer coefficient between the solid and gas phases.
6. The self-heat method of thermal conductivity measurement is a relatively easy and expedient way to measure the thermal conductivity of heat source materials and is capable of

achieving errors of less than 5% if the dimensions of the thermal conductivity cell and the thermocouples are properly selected, and boundary conditions are monitored.

References

- [1] T. K. Keenan, R. A. Kent, R. W. Zocher, USAEC Report LA-5622-MS, Los Alamos Scientific Laboratory (1974).
- [2] G. Ondracek, and B. Schulz, J. Nucl. Mater. 46 (1973) 253.
- [3] V. J. Tennery, J. Nucl. Mater. 54 (1974) 73.
- [4] D. A. G. Bruggeman, Ann. Physik 24 (1935) 636.
- [5] J. C. Van Craeynest and J. C. Weilbacker, J. Nucl. Mater. 26 (1968) 132.
- [6] R. L. Gibby, USAEC Report BNWL-704, Battelle Laboratories (1968).
- [7] J. F. Lagedrost, D. F. Askey, V. W. Storhok, and J. E. Gates, Nucl. Applic. 4 (1968) 54.
- [8] O. L. Kruger and H. Savage, J. Chem. Phys., 49 (1968) 4540.
- [9] J. C. Maxwell, Treatise on Electricity and Magnetism, Vol. 1 (Oxford University Press, Oxford, 1873) p. 104.
- [10] D. A. G. Bruggeman, Ann. Physik 25 (1936) 645, Series 6.
- [11] W. Niesel, Ann. Physik 10 (1952) 336, Series 6.
- [12] W. E. Baily, D. P. Hines, and E. L. Zebroski, Trans. Amer. Nucl. Soc., 8, (1965) 39.
- [13] V. Whatley, Savannah River Laboratory, personal communication.
- [14] Y. S. Touloukian, P. E. Liley, and S. C. Saxena, eds., Thermophysical Properties of Matter: Vol. 3 Thermal Conductivity of Non-Metallic Liquids and Gases (Plenum Press, New York, 1970).

TABLE 1. Thermal Conductivity of High Density PuO₂^a

Temp., °C	Density, ^b g/cm ³	Specific Heat, ^c cal/g-°C	Thermal Diffusivity, ^b cm ² /sec	Thermal Conductivity for 96% Td, cal/sec-cm-°C	Calculated ^d Thermal Conductivity for 100% TD, cal/sec-cm-°C
SAMPLE G 3 - 1					
300	10.98	0.0765	0.0181	0.0152	0.0160
400	10.95	0.0780	0.0145	0.0124	0.0131
500	10.91	0.0792	0.0119	0.0103	0.0108
600	10.88	0.0801	0.0100	0.00871	0.0092
700	10.83	0.0807	0.0085	0.00743	0.0078
800	10.80	0.0811	0.0076	0.00666	0.0070
900	10.73	0.0814	0.0070	0.00611	0.0064
1000	10.70	0.0817	0.0067	0.00586	0.0062
1100	10.67	0.0819	0.0065	0.00568	0.0060
SAMPLE G 3 - 2					
300	10.98	0.0765	0.0195	0.0164	0.0173
400	10.95	0.0780	0.0158	0.0135	0.0142
500	10.91	0.0792	0.0128	0.0111	0.0117
600	10.88	0.0801	0.0105	0.00915	0.0096
700	10.83	0.0807	0.0089	0.00778	0.0082
800	10.80	0.0811	0.0079	0.00692	0.0073
900	10.73	0.0814	0.0073	0.00638	0.0067
1000	10.70	0.0817	0.0070	0.00612	0.0065
1100	10.67	0.0819	0.0068	0.00594	0.0063
1200	10.63	0.0821	0.0066	0.00575	0.0061

a. Assumed molecular weight of 271 g/mole; recalculated from data cited in Reference 7.

b. Reference 7.

c. Reference 8.

d. Maxwell's Equation used to determine correction factor.

TABLE 2. Thermal Conductivity of PuO₂^a (81.9% Theoretical Density in Vacuum)

<i>Temp., °C</i>	<i>Density,^b g/cc</i>	<i>Specific Heat,^c cal/g-°C</i>	<i>Thermal Diffusivity,^b cm²/sec</i>	<i>Thermal Conductivity, cal/sec-cm-°C</i>
SAMPLE G 5 - 1				
200	9.34	0.0741	0.0210	0.0145
300	9.30	0.0765	0.0167	0.0119
400	9.27	0.0780	0.0137	0.0099
500	9.25	0.0792	0.0115	0.0084
600	9.22	0.0801	0.0100	0.0081
700	9.18	0.0807	0.0088	0.0065
800	9.15	0.0811	0.0080	0.0059
900	9.10	0.0814	0.0074	0.0055
1000	9.07	0.0817	0.0069	0.0051
1100	9.04	0.0819	0.0065	0.0048
1200	9.00	0.0821	0.0062	0.0046
1300	8.98	0.0822	0.0058	0.0043
1360	8.96	0.0824	0.0054	0.0040
SAMPLE G 5 - 2				
300	9.30	0.0765	0.0170	0.0121
400	9.27	0.0780	0.0137	0.0099
500	9.25	0.0792	0.0118	0.0086
600	9.22	0.0801	0.0103	0.0083
700	9.18	0.0807	0.0091	0.0067
800	9.15	0.0811	0.0082	0.0061
900	9.10	0.0814	0.0076	0.0056
1000	9.07	0.0817	0.0073	0.0054
1100	9.04	0.0819	0.0071	0.0053
1200	9.00	0.0821	0.0068	0.0050
1300	8.98	0.0822	0.0060	0.0044
1360	8.96	0.0824	0.0050	0.0037

a. Assumed molecular weight of 271 g/mole; 81.9% of theoretical density in vacuum.

b. Reference 7.

c. Reference 8.

TABLE 3. Comparison of Measured and Calculated^a Temperatures for Hot-Pressed Spheres

<i>Gas</i>	<i>Center Temperature, °C</i>	<i>Surface Temperature, °C</i>	
		<i>Measured^b</i>	<i>Calculated</i>
Helium	460	300	339
Helium	1084	1000	981
Argon	497	300	-503
Argon	1063	1000	398

a. Calculated from Series Slab Model.

b. Reference 3.

TABLE 4. Temperature Data for Fixed Thermocouple Measurements

A. Ball-Milled Powder: $\rho = 3.55$ g/cc, $R = 1.536$ cm, $S_0 = 0.339$ cal/sec-cm³

Air		Helium		Argon #1		Argon #2	
T_s	T_c	T_s	T_c	T_s	T_c	T_s	T_c
246	605	181	364	188	538	190	530
371	718	189	368	350	698	189	539
447	790	352	541	432	774	354	691
541	878	440	631	524	862	442	770
628	956	522	714	611	944	528	849
715	1018	189	372	695	1023	611	927
		615	810	785	1103	699	1000
		702	899			792	1094
		788	980				

B. Ball Milled Powder: $\rho = 3.07$ g/cc, $R = 1.667$ cm, $S_0 = 0.294$ cal/sec-cm³

Air		Helium		Argon	
T_s	T_c	T_s	T_c	T_s	T_c
216	242	222	451	244	720
376	877	220	452	247	726
323	843	372	615	246	724
278	804	462	704	247	724
289	812	547	787	390	849
409	907	706	945	471	918
476	954			563	994
555	1004			714	1119
736	1100				
240	642				

C. As-Calcined Powder: $\rho = 1.2$ g/cc, $R = 1.746$ cm, $S_0 = 0.115$ cal/sec-cm³

Air		Argon	
T_s	T_c	T_s	T_c
129	411	136	476
161	440		
292	543		

D. As-Calcined Powder: $\rho = 1.12$ g/cc, $R = 1.774$ cm, $S_0 = 0.107$ cal/sec-cm³

Air	
T_s	T_c
100	401
139	436
295	559

E. High Internal Density Granules^a: $\rho = 6.24$ g/cc, $R = 1.27$ cm, $S_0 = 0.597$ cal/sec-cm³

Air		Argon		Helium		Vacuum ^b	
T_s	T_c	T_s	T_c	T_s	T_c	T_s	T_c
125	334	165	435	108	205	207	954
$\Delta T = 209^\circ\text{C}$		$\Delta T = 270^\circ\text{C}$		$\Delta T = 97^\circ\text{C}$		$\Delta T = 747^\circ\text{C}$	

a. In aluminum cylinder with spherical cavity.

b. Mechanical pump; estimated pressure = 1000 μm of mercury (1 Torr).

TABLE 5. Thermocouple Error in Terms of Diameter

<i>Thermocouple Diameter, in.</i>	<i>Approximate Error, %</i>
0.003	1.5
0.005	4
0.008	10

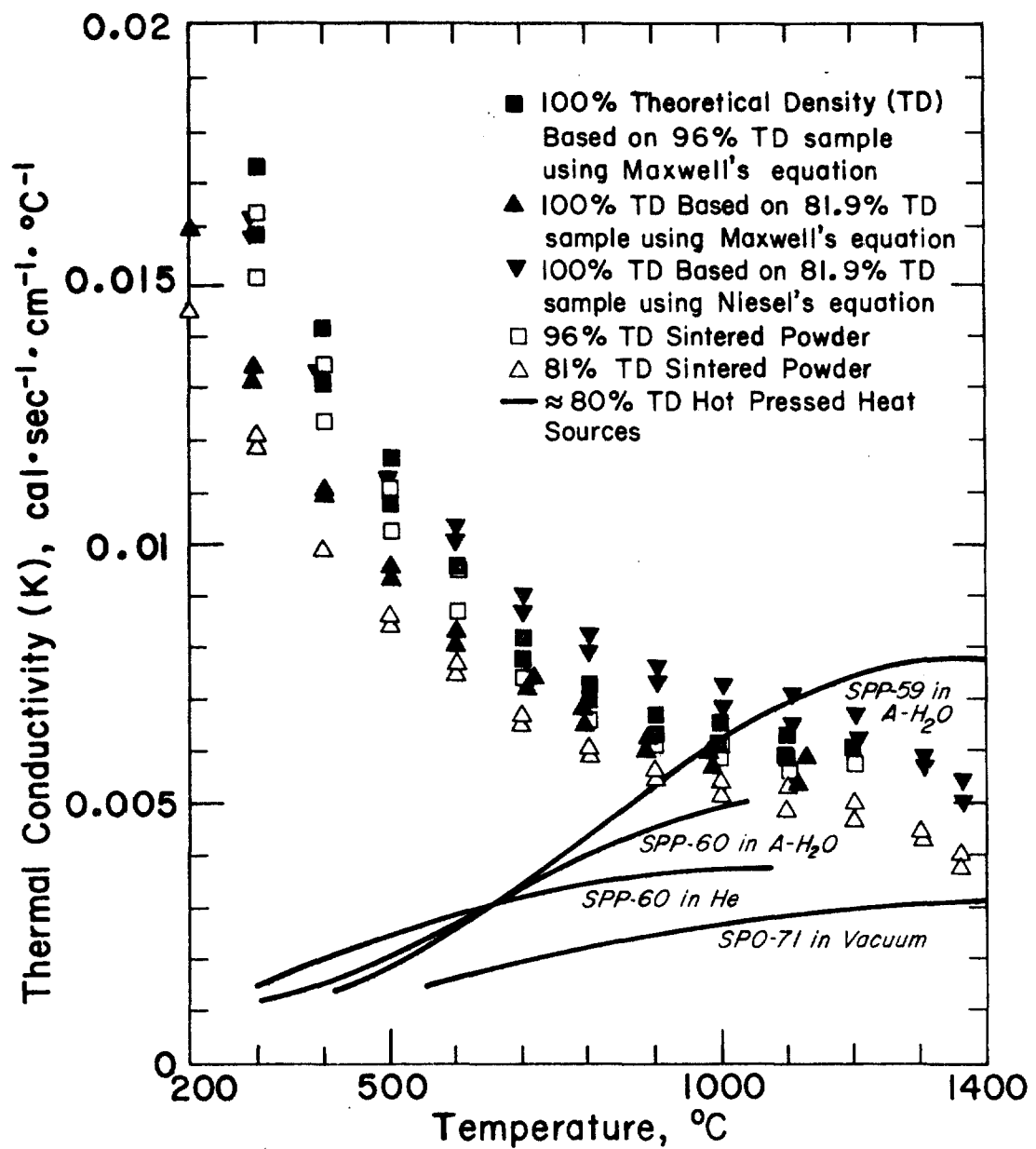


FIG. 1. Thermal Conductivity of Dense PuO₂

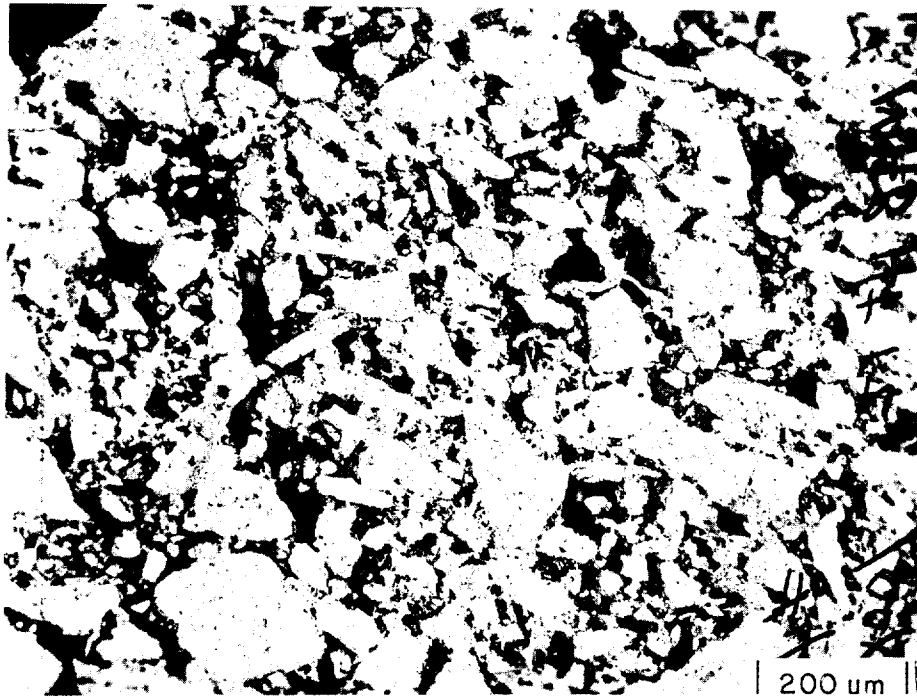


FIG. 2. Microstructure of 82% PuO₂ Hot-Pressed from Calcined Oxalate Granules

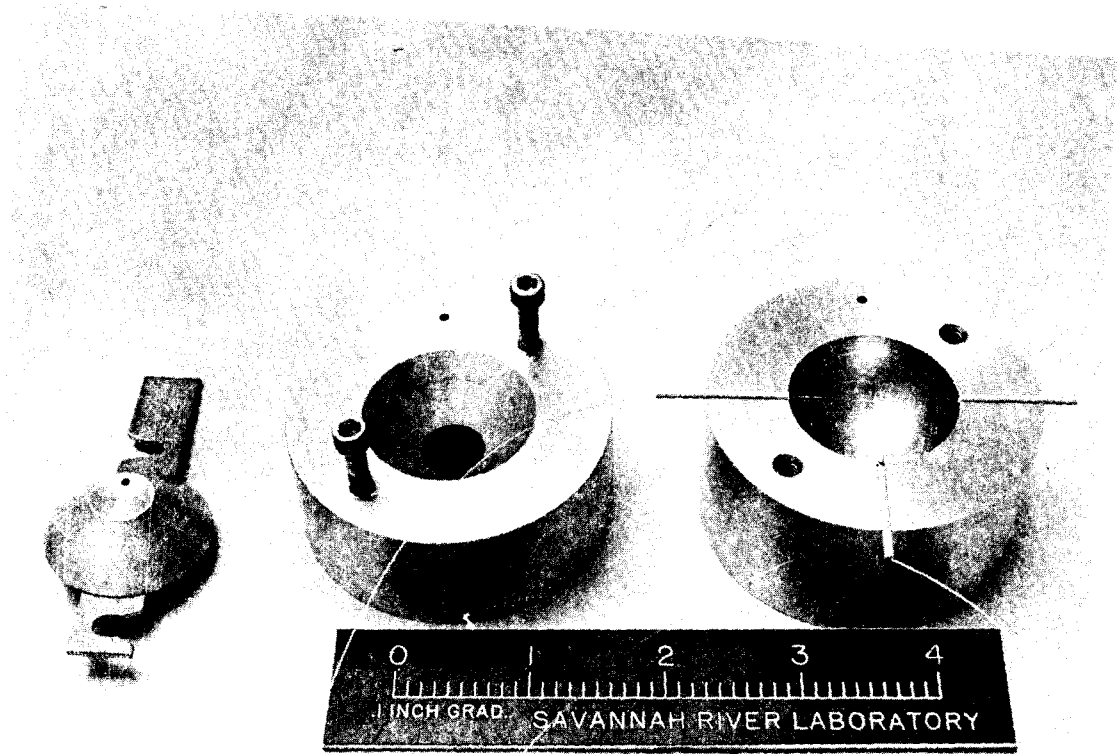


FIG. 3. Aluminum Thermal Conductivity Cell
(Movable Thermocouple Method)

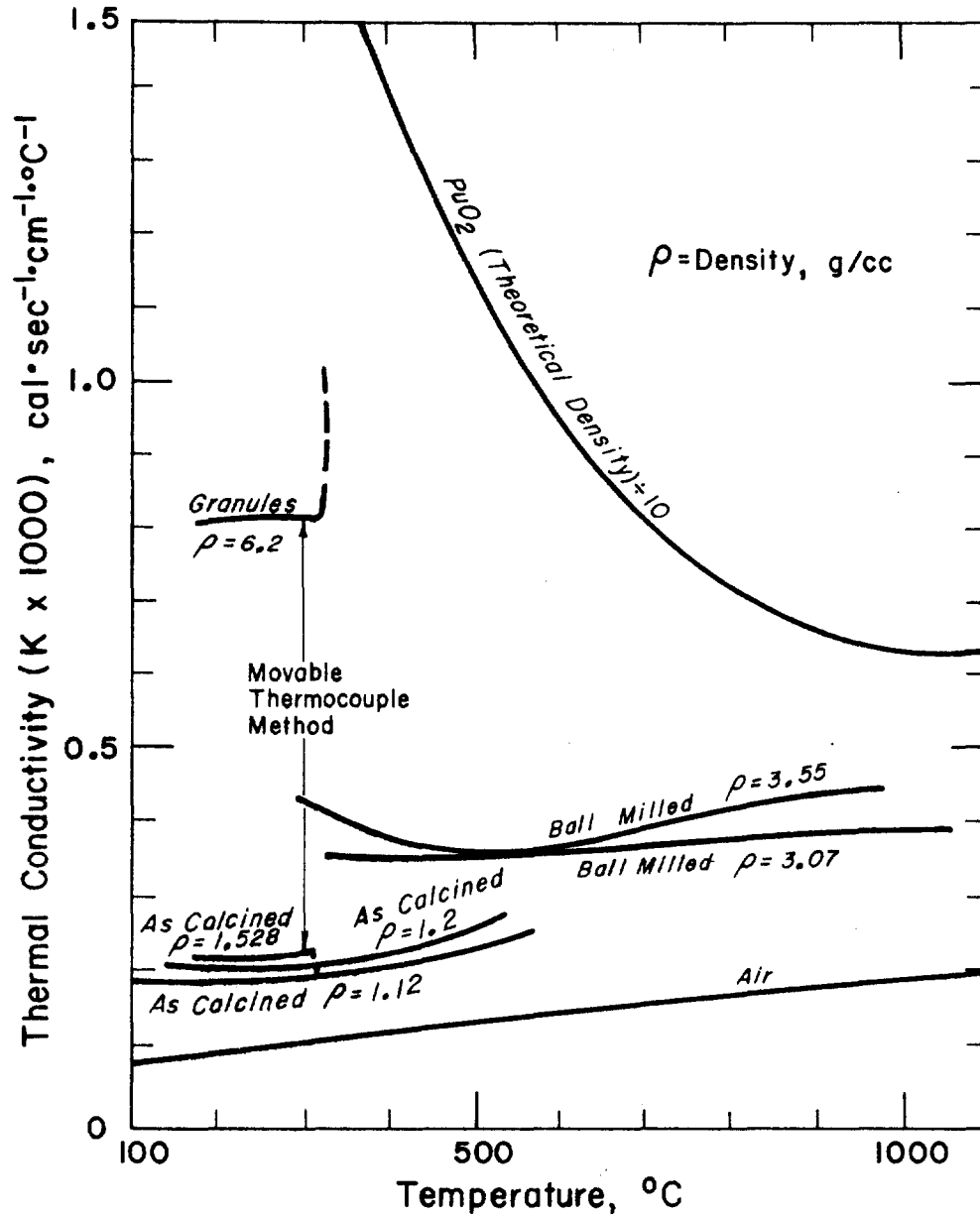


FIG. 4. Thermal Conductivity of PuO₂ Powder in Argon

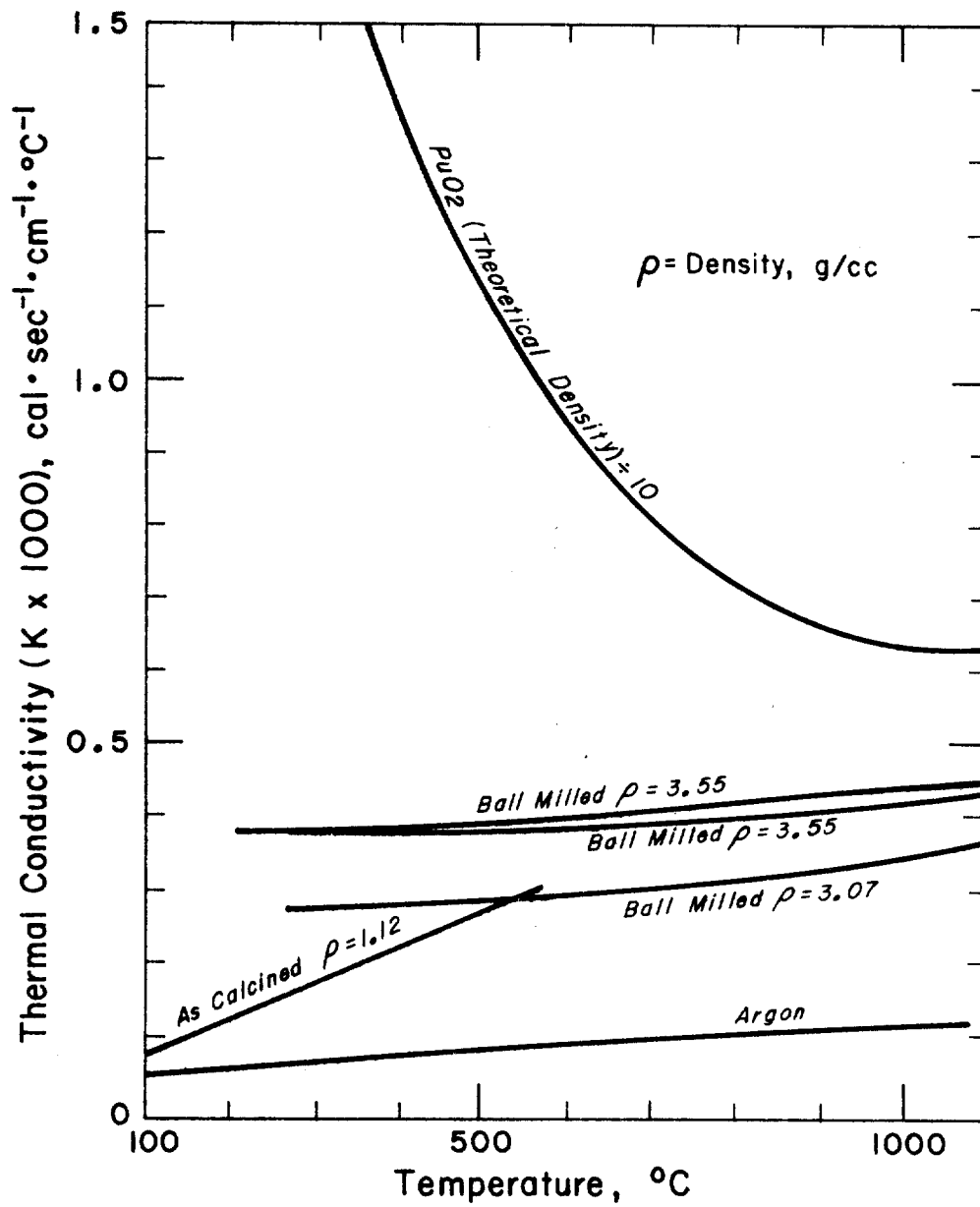


FIG. 5. Thermal Conductivity of PuO_2 Powder in Air

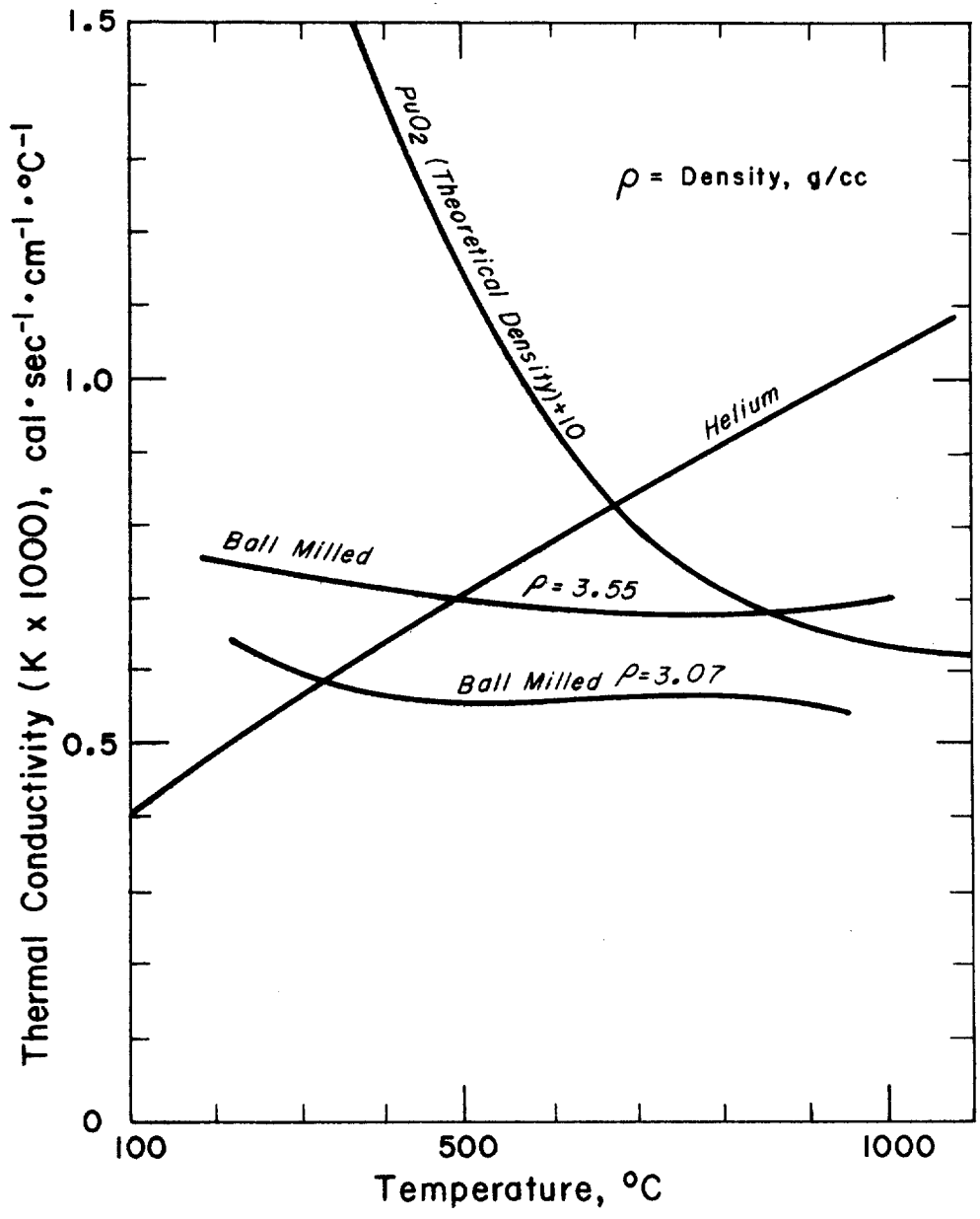


FIG. 6. Thermal Conductivity of PuO₂ Powder in Helium

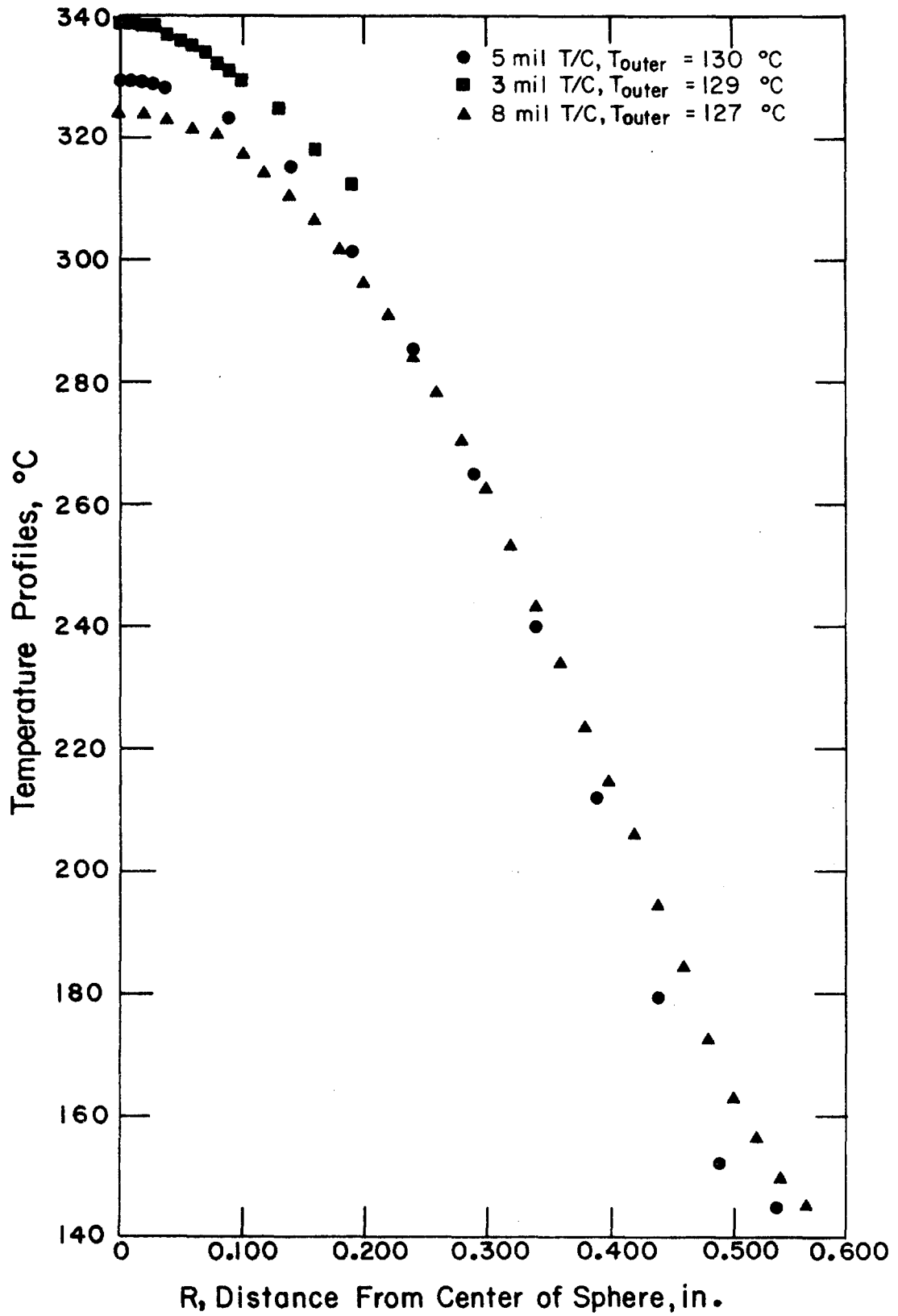


FIG. 7. Effect of Thermocouple Diameter on Measured Temperature Profile of PuO_2 Granules in Air